

A Unique Discrete Tetranuclear Cu'–Cu(N-N)₂Cu–Cu' Copper(II) Complex, Built from a μ_3 -1,2,4-Triazolato- μ -carboxylato Ligand, as an Effective DNA Cleavage Agent

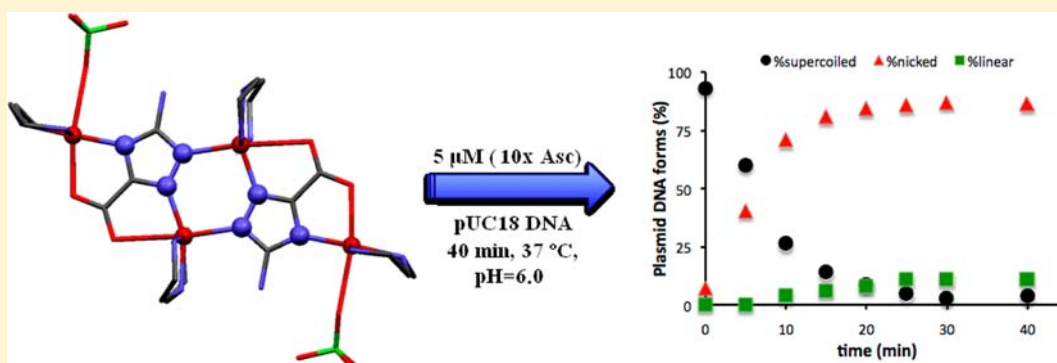
Javier Hernández-Gil,[†] Sacramento Ferrer,^{*†} Alfonso Castiñeiras,[‡] and Francesc Lloret[§]

[†]Departament de Química Inorgànica, Universitat de València, Vicent Andrés Estellés s/n, 46100-Burjassot, Valencia, Spain

[‡]Departamento de Química Inorgànica, Universidad de Santiago de Compostela, Campus Universitario Sur, E-15782 Santiago de Compostela, Spain

[§]Institut de Ciència Molecular, Universitat de València, Catedràtic José Beltrán 2, 46980-Paterna, Valencia, Spain

Supporting Information



ABSTRACT: The title compound, characterized by means of an X-ray structure analysis, represents an easy example of a noncatena “1 + 2 + 1” tetranuclear copper(II) μ_3 -triazolate compound. $[\text{Cu}_4(\text{atc})_2(\text{dien})_4(\text{ClO}_4)_2](\text{ClO}_4)_2 \cdot 2\text{H}_2\text{O}$ (**1**), where $\text{H}_2\text{atc} = 5\text{-amino-1,2,4-triazole-3-carboxylic acid}$ and $\text{dien} = \text{diethylenetriamine} = 1,4,7\text{-triazahexane}$, contains two copper atoms linked by a double diazinic bridge, each of which is further connected to a third and fourth copper atom (Cu') through the triply bridging triazolato ring and the bidentate carboxylato group of the atc^{2-} ligands. The copper–copper distances within the tetranuclear unit are $\text{Cu–Cu} = 4.059 \text{ \AA}$, $\text{Cu–Cu}' = 5.686$ and 6.370 \AA , and $\text{Cu}'\text{–Cu}' = 11.373 \text{ \AA}$. The compound self-assembles into a tridimensional hydrogen-bonded network to generate a MOF. **1** exhibits antiferromagnetic behavior with $g = 2.10(1)$, $J = -34.1(2) \text{ cm}^{-1}$ and $j = -5.50(3) \text{ cm}^{-1}$, where J is the coupling constant of the central Cu–Cu pair and j the coupling constant of the two $\text{Cu–Cu}'$ ($\text{Cu}_{\text{central}}\text{–Cu}_{\text{peripheral}}$) pairs, as defined by $\mathbf{H} = -J \mathbf{S}_2\mathbf{S}_{2a} - j (\mathbf{S}_1\mathbf{S}_2 + \mathbf{S}_{2a}\mathbf{S}_{1a})$. Complex **1** has been tested as nuclease mimic. It shows good binding propensity to calf thymus DNA, with a binding constant value of $6.20 \times 10^6 \text{ M}^{-1}$ (K_{app}) and $\Delta T_m = 18.3 \text{ }^\circ\text{C}$. Moreover, the compound displays efficient oxidative cleavage of pUC18 DNA, even at low concentration, in the presence of a mild reducing agent (ascorbate), with a rate constant for the conversion of supercoiled to nicked DNA (k_{obs}) of $\sim 0.126 \text{ min}^{-1}$. The good reactivity of **1** toward DNA is explained from the electrostatic interactions of the cationic species produced in solution.

INTRODUCTION

The design of small compounds able of catalyzing DNA scission at physiological conditions is of great interest for biotechnological applications and the development of novel therapeutic agents. Transition-metal complexes (especially of essential iron and copper) in their reduced oxidation state can promote the formation of free radicals through Haber–Weiss or Fenton reactions that can oxidize several biomolecules.^{1–3} Based on this property, much effort has been undertaken by different groups to prepare complexes of transition metals capable of binding and breaking the DNA double helix. Several well-known and best-characterized nucleolytic agents are $[\text{Fe}(\text{EDTA})]^{2-}$ ($\text{EDTA} = \text{ethylenediaminetetraacetic acid}$),^{4a}

$[\text{Cu}(\text{OP})_2]^+$ ($\text{OP} = 1,10\text{-phenanthroline}$),^{4b} Fe-BLM ($\text{BLM} = \text{bleomycin}$),^{4c} Ni-peptides ,^{4d} and metal-salen [$\text{salen} = N,N'$ -ethylene-bis(salicylideneaminato)].^{4e} The intrinsic redox properties of $\text{Cu}(\text{II})$ have allowed the obtention of a series of copper complexes that induce DNA cleavage through an oxidative mechanism from a wide diversity of ligands including triazole derivatives.^{1,5,6} Our group described the nuclease ability of two copper-triazole compounds of the same ligand, $[\text{Cu}(\text{Hapt})]^{2+}$ and $[\text{Cu}(\text{Hapt})_2]^{2+}$ ($\text{Hapt} = 5\text{-amino-3-pyridyl-1,2,4-triazole}$), which showed different activity and differences in the ROS

Received: June 1, 2012

Published: August 31, 2012

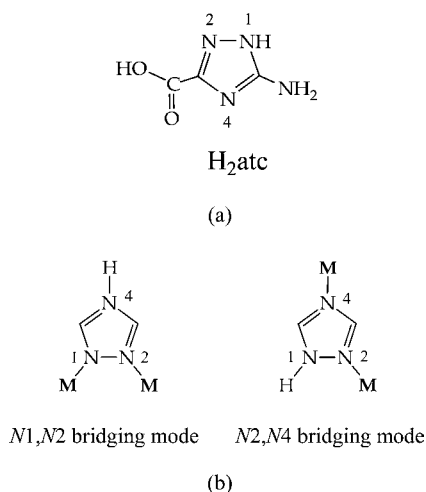


species involved in the DNA strand scission mechanism.⁷ Furthermore, prior to this work, other authors reported on the antiproliferative activity toward neoplastic cells of another couple of copper-triazole complexes, *cis*-[CuCl₂(H₂L1)]Cl and *cis*-[CuCl₂(L2)], where HL1 = 1,4-dihydro-4-amino-3-(2-pyridyl)-5-thioxo-1,2,4-triazole and L2 = 4-amino-5-methylthio-3-(2-pyridyl)-1,2,4-triazole.⁸

The above-mentioned compounds are typically mononuclear complexes. Recently, multinuclear complexes have acquired importance since Karlin et al. showed that nuclearity is a crucial parameter in the mechanism of the oxidative cleavage due to the possible synergy between metallic centers, given that it can facilitate the formation of the active intermediate.⁹ Some dinuclear and trinuclear copper complexes have been investigated as good DNA cleavage agents,¹⁰ among them, the dinuclear copper(II) triazole [Cu₂L3(μ-SO₄)](PF₆)₂ {L3 = 3,5-bis[bis(pyridine-2-ylmethyl)amino)methyl]-4-amino-1,2,4-triazole} complex, which has been reported to promote single and double strand DNA cleavage in both aerobic and anaerobic conditions.¹¹

In this context, we have selected the small H₂atc ligand (H₂atc = 5-amino-1,2,4-triazole-3-carboxylic acid) (Scheme 1a),

Scheme 1



with several bridging and chelating possibilities, especially in its anionic atc²⁻ form, as a way of producing multinuclear copper structures that could serve as efficient oxidative nucleases through introducing several positively charged centers in the metallonuclease that could enhance the affinity toward the negatively charged DNA molecule.¹ In the presence of dien (dien = diethylenetriamine), we have succeeded in obtaining a *soluble*, simple tetranuclear complex, which is described and tested in this work.

Tetranuclear copper(II) coordination compounds show a variety of structures. The classical review by Haasnoot,^{12a} that by Brooker et al.,^{12b} and the recent work by Gámez et al.^{12c} reveal that the group of 1,2,4-triazole copper compounds with four metal atoms is very reduced. These complexes can be classified in four groups: (i) *tetrahedral*, (ii) *rectangular*, (iii) *butterfly*, and (iv) the “1 + 2 + 1” type.

(i) Only one atypical Cu(II) cluster, the complex [Cu(HL4)(H₂O)]₄(NO₃)₄ (HL4 = 3-(pyridin-2-yl)-5-(pyrazin-2-yl)-1,2,4-triazole),¹³ has been described with a *tetrahedral* arrangement of the coppers. The structural

role played by the heterocycle in this case is not relevant, in contrast with what happens with cubane or cubane-stepped compounds built from μ-oxido, μ-alkoxide, or μ-halo ligands.¹⁴

- (ii) A few *rectangular* examples, which can be regarded as *dimers* of N1,N2-bridged *dinuclear units* (Cu₂...Cu₂), have been reported, being among them the [Cu^I₂Cu^{II}₂(L5)₄(pic)₂] and the [Cu^I₄(L5)₄] (L5 = 3,5-bis-(pyridin-2-yl)-1,2,4-triazole, Hpic = picolinic acid = pyridine-2-carboxylic acid) compounds,^{15a,b} both obtained from hydrothermal synthesis. The latter is actually the tetrameric block of a supramolecular structure, with the four metal centers of the block defining a quasi-rectangle (Cu1...Cu2 = 4.325 Å, Cu1–Cu2A = 5.972 Å, Cu2...Cu1...Cu2A = 90.7°). Another rectangular complex is [Cu₄(L6)₄(OH)₂(NO₃)(H₂O)₆](NO₃) (HL6 = 3,5-diamino-1,2,4-triazole = guanazole),^{15c} which exhibits two types of Cu...Cu bridges; one involves only the [–N–N–] moiety of a guanazole ligand, and the other exhibits this motif together with a μ–OH[–] bridge.
- (iii) In the literature, some structures with the so-called *butterfly* topology can also be found. This organization consists of two fused oxo or hydroxo-centered triangles, usually exhibiting additional bridging carboxylate ligands; the two central metal ions form the “body” of the butterfly and the remaining two external metals constitute the wings.^{12c} The complexes [Cu₄(OH)₂(L7)₂(piv)₆] and [Cu₄(OH)₂(L8)₂(piv)₆ (L7 = 4-amino-3,5-dimethyl-1,2,4-triazole, L8 = 4-*t*-butyl-1,2,4-triazole, Hpiv = pivalic acid) belong to this category.¹⁶
- (iv) Very recently, in 2012, Brooker and co-workers^{17a} have published a tetranuclear Cu(II) structure with triazole ligands, namely, [Cu^{II}₄(L3)₂(H₂O)₂(BF₄)₂](BF₄)₆·CH₃CN [L3 = see above], which contains a novel “1 + 2 + 1” copper arrangement (Cu...Cu₂...Cu versus Cu₂...Cu₂); these authors have also reported on the analogous [Cu^{II}₄(L3')₂(H₂O)₂(μ-F)₂](BF₄)₆·0.5H₂O {L3' = 3,5-bis[bis(2-pyridylmethyl)aminomethyl]-4-phenyl-1,2,4-triazole} compound, although no crystals of it were obtained.

The compound of this work represents, to the best of our knowledge, the second example of this novel (iv) type of tetranuclear copper(II) compounds.^{17b} It comprises a planar Cu₄ group, planarity imposed by the μ₃-triazolato ligand, with both “short” (diatomic) and “long” (triatomic) bridges. With related bridging systems (N4-unsubstituted 1,2,4-triazole derivatives) only polymers have been reported since the N2,N4 bridging mode of the triazoles usually leads to two-dimensional, layered, compounds (Scheme 1a and 1b).^{12a,15a,18} In this work, we first study its synthesis, structure, and spectroscopic and magnetic characterization, and then its DNA binding and DNA cleavage properties.

EXPERIMENTAL SECTION

Materials and Chemicals. H₂atc was supplied by Panreac (Panreac Química S.A.U., Barcelona, Spain). All other chemicals and solvents were of reagent or analytical grade, and were used as received unless otherwise indicated. Plasmid pUC18 (0.25 μg/μL, 750 μM in nucleotides) in TE (Tris 10 mM and EDTA 1 mM, pH 8.0) was purchased from Roche Diagnostics, Germany. Calf thymus DNA (CT DNA), type XV, was obtained from Sigma.

Instrumentation and Methods. Elemental analyses were performed with a CE Instrument EA 1110 CHNS analyzer. Infrared spectra were recorded as KBr disks using a Mattson Satellite FTIR spectrophotometer from 4000 cm^{-1} to 400 cm^{-1} . UV–vis spectra in solution were recorded with an Hewlett-Packard (Model HP 8453 spectrophotometer), of solid samples, with a T90 Plus spectrophotometer equipped with a Model IS19-1 integrating sphere. Low-resolution electrospray ionization mass spectrometry (ESI-MS) analysis in positive mode was performed on a Bruker Esquire 3000 plus LC-MS system; high-resolution ESI-MS in positive mode on an ABS Giex Triple TOF 5600. Electronic paramagnetic resonance (EPR) spectra of molten crystals were collected with a Bruker ELEXSYS spectrometer operating at X-band frequency in the temperature range of 10–300 K. Magnetic susceptibility measurements on polycrystalline samples were carried out with a Superconducting Quantum Interference Design (SQUID) magnetometer in the temperature range of 1.9–300 K. Diamagnetic corrections of the constituent atoms were estimated from Pascal's constants. Experimental susceptibilities were also corrected for the temperature-independent paramagnetism ($60 \times 10^{-6} \text{ cm}^3 \text{ mol}^{-1}$ per copper(II)) and for the magnetization of the sample holder.

Synthesis. $[\text{Cu}_4(\text{atc})_2(\text{dien})_4(\text{ClO}_4)_2](\text{ClO}_4)_2 \cdot 2\text{H}_2\text{O}$ (**1**). The ligand H_2atc (137 mg, 1 mmol) was suspended in 2 mL of an aqueous sodium hydroxide solution (40 mg, 1 mmol). The ligand was partially solvated. To this suspension, first 40 mL of water, and, afterward, 0.21 mL of diethylenetriamine (2 mmol, $\rho = 0.95 \text{ g/mL}$) were added (the amine, dropwise from a micropipet) with continuous stirring; full solution of the ligand was thus reached almost immediately. Then, crystals of $\text{Cu}(\text{ClO}_4)_2 \cdot 6\text{H}_2\text{O}$ (700 mg, 2 mmol) were slowly added (in ca. 5 portions over 2 min) while stirring (the Cu salt crystals were dissolved as added). The resulting dark blue solution was maintained under stirring. After ca. 15 min, some turbidity was observed. The (scarce) light blue precipitate was removed by filtration and the dark blue solution kept covered with Parafilm in a crystallizing dish at 4 °C (the reactants ratio is $\text{H}_2\text{atc}:\text{NaOH}:\text{dien}:\text{Cu(II)} = 1:1:2:2$). Dark “electric”-blue lens-shaped crystals suitable for X-ray analysis of **1** were obtained after ca. 12 months. Yield: ca. 1.5 g (ca. 80%). When the final dark blue solution was allowed to slowly evaporate at room temperature instead, a microcrystalline product corresponding to compound **1** appeared within 1.5–2 months. Yield: ca. 1.7 g (ca. 90%). Microanalysis (performed on single crystals): Calcd. for $\text{C}_{22}\text{H}_{60}\text{Cl}_4\text{Cu}_4\text{N}_{20}\text{O}_{22}$ (1352.86): C, 19.53; H, 4.77; N, 20.71. Found: C, 19.78; H, 4.70; N, 21.02. Selected FT-IR data (KBr pellet) $\tilde{\nu}_{\text{max}}$ (cm^{-1}): $[\nu(\text{O}-\text{H}) + \nu(\text{N}-\text{H})]$ 3530 w, 3351–3300 d-s, 3170 w, 3090 w; $[\nu(\text{COO})_{\text{asym}}]$ 1631 s, 1601 sh; $[\delta(\text{N}-\text{H}) + \nu(\text{C}=\text{N})_{\text{ring}} + \nu(\text{C}=\text{C})_{\text{ring}}]$ 1593 sh, 1526 sh, 1510 sh; $[\nu(\text{COO})_{\text{sym}}]$ 1469 s; $[\nu(\text{ClO}_4)]$ 1141 sh, 1093 vs, 1050 sh, 1021 sh. UV–vis (solid): λ_{max} (nm): 610; UV–vis (H_2O): λ_{max} ($\text{M}^{-1} \text{ cm}^{-1}$): 615 [225], 246 [15200]. Conductivity measurements (H_2O , 10^{-3} M): 380 ($\Omega^{-1} \text{ cm}^2 \text{ mol}^{-1}$); in the same experimental conditions the control electrolyte $\text{Cu}(\text{NO}_3)_2 \cdot 3\text{H}_2\text{O}$: 343 ($\Omega^{-1} \text{ cm}^2 \text{ mol}^{-1}$).

[Caution!] Although no problems were encountered in this work, perchlorate salts are potentially explosive. They should be prepared in small quantities and handled with care.

X-ray Crystallography. A blue plate crystal of $[\text{Cu}_4(\text{atc})_2(\text{dien})_4(\text{ClO}_4)_2](\text{ClO}_4)_2 \cdot 2\text{H}_2\text{O}$ (**1**) was mounted on a glass fiber and used for data collection. Crystal data were collected at 100.0(1) K, using a Bruker X8 Kappa APEXII diffractometer. Graphite monochromated Mo $K\alpha$ radiation ($\lambda = 0.71073 \text{ \AA}$) was used throughout. The data were processed with APEX2¹⁹ and corrected for absorption using SADABS (transmission factors: 1.000–0.808).²⁰ The structure was solved by direct methods using the program SHELXS-97²¹ and refined by full-matrix least-squares techniques against F^2 using SHELXL-97.²² Positional and anisotropic atomic displacement parameters were refined for all nonhydrogen atoms. The geometry of the ClO_4^- ligand is imposed by a pseudo-mirror plane which contains the Cl(1)–O(13) bond with 0.5 occupancy for each atom. The ClO_4^- anion appeared to occur in two positions related by a pseudo-mirror plane. From the refined multiplicities of the O and O* atoms, the occupancy factors for the two orientations were found to be 0.50 each.

Hydrogen atoms bonded to carbon were placed geometrically, and the O–H and N–H hydrogen atoms were initially positioned at sites determined from difference maps, but the positional parameters of all H atoms were included as fixed contributions riding on attached atoms. Atomic scattering factors were taken from “International Tables for Crystallography”.²³ Molecular graphics performed with DIAMOND.²⁴ Crystal data: $\text{C}_{22}\text{H}_{60}\text{Cl}_4\text{Cu}_4\text{N}_{20}\text{O}_{22}$, $M = 1352.86$, monoclinic, $C 2/m$, $a = 24.1332(6) \text{ \AA}$, $b = 8.4915(2) \text{ \AA}$, $c = 14.2128(3) \text{ \AA}$, $\beta = 121.9540(10)^\circ$, volume = $2471.25(10) \text{ \AA}^3$, $Z = 2$, $D_c = 1.818 \text{ mg/cm}^3$, $F(000) = 1384$; 2922 unique reflections; final R indices [$I > 2\sigma(I)$]: $R_1 = 0.0400$, $\omega R_2 = 0.0940$; R indices (all data): $R_1 = 0.0481$, $\omega R_2 = 0.0980$ (Table S1). Cambridge Crystallographic Data Centre (CCDC) File No. 885464 (1) contains the supplementary crystallographic data for this paper. These data can be obtained free of charge from The CCDC at www.ccdc.cam.ac.uk/data_request/cif.

Crystallographic literature revision was performed with the help of CSD-Conquest.²⁵

DNA–Copper Complex Interaction Studies. The fluorescence spectra were recorded with a JASCO FP-6200 spectrofluorometer at room temperature. Ethidium bromide (EB) was used as a reference to determine the relative DNA binding properties of complex **1** to calf thymus DNA (CT-DNA). The experiments entailed the addition of copper(II) complex solutions at final concentrations ranging from 0 to 50 μM to samples containing 50 μM bp CT-DNA and 50 μM EB in cacodylate buffer (0.1 M, pH 6.0). All of samples were excited at 500 nm, and emission was recorded between 530 nm and 650 nm.

For competitive ethidium displacement assays, a working solution containing 3 μM CT-DNA ($\epsilon_{260} = 6600 \text{ M}(\text{bp})^{-1} \text{ cm}^{-1}$), along with 3.78 μM EB in cacodylate buffer (0.1 M, pH 6.0) was prepared. Complex **1**, Hoechst 33258, Methyl Green, CuSO_4 and acridine were prepared at 0.5 mM in cacodylate buffer (0.1 M, pH 6.0). Excitation and emission wavelengths were set to 500 and 595 nm, respectively. The apparent binding constants were calculated using $K_{\text{app}} = K_{\text{EB}} \times (3.78/\text{C}_{50})$ where $K_{\text{EB}} = 3 \times 10^7 \text{ M}(\text{bp})^{-1}$. We calculated this K_{EB} value (pH 6.0), following procedures given in the literature.^{26,27a,b}

DNA-melting experiments were carried out by monitoring the absorbance spectrum between 1000 and 200 nm of calf thymus DNA (100 μM bp) at different temperatures both in the absence and the presence of the complex, in ratios from 8:1 to 2:1 $[\text{DNA}]/[\text{complex}]$. Measurements were carried out with an Agilent 8453 UV–vis spectrophotometer equipped with a Peltier temperature-controlled sample cell and driver (Agilent 89090A). The solution containing the complex and CT-DNA in phosphate buffer (pH 7.2, 1 mM phosphate, 2 mM NaCl) was stirred continuously and heated with a temperature increase rate of 1 °C min^{-1} . The temperature interval studied ranged from 25 °C to 90 °C. The melting point was obtained with the first derivative.

Viscosity measurements were performed using a semimicro Ubbelohde viscosimeter, maintained at a constant temperature of 25.0 ± 0.1 °C in a Julabo ME16G thermostatic bath. Solutions of the complex (final concentrations ranging from 1 to 10 μM) in cacodylate buffer (0.1 M, pH 6.0) were added to a solution of CT-DNA (50 μM bp) in cacodylate buffer. The flow times were measured in triplicate with a stopwatch. Data were presented as $(\eta/\eta_0)^{1/3}$ versus the ratio of the complex concentration to DNA, where η is the viscosity of the DNA in the presence of the complex and η_0 is the viscosity of the DNA alone. Viscosity values were calculated from the observed flow time of a DNA-containing solution corrected from the flow time of buffer alone (t_0), $\eta = t - t_0$.

DNA Cleavage Experiments. The cleavage of plasmid DNA was monitored by agarose gel electrophoresis. Complex and activating agent stock solutions were prepared in cacodylate buffer (0.1 M, pH 6.0). Reactions were performed by mixing 7 μL of cacodylate buffer (0.1 M, pH 6.0), 6 μL of complex solution (with final concentrations of 5, 10, 20, and 40 μM), 1 μL of pUC18 DNA solution (0.25 $\mu\text{g}/\mu\text{L}$, 750 μM bp), and 6 μL of activating agent solution (sodium ascorbate) in a 2.5-fold excess relative to compound concentration, equivalent to (2.5/4)-fold relative to copper concentration, both in compound **1** and in control salt.

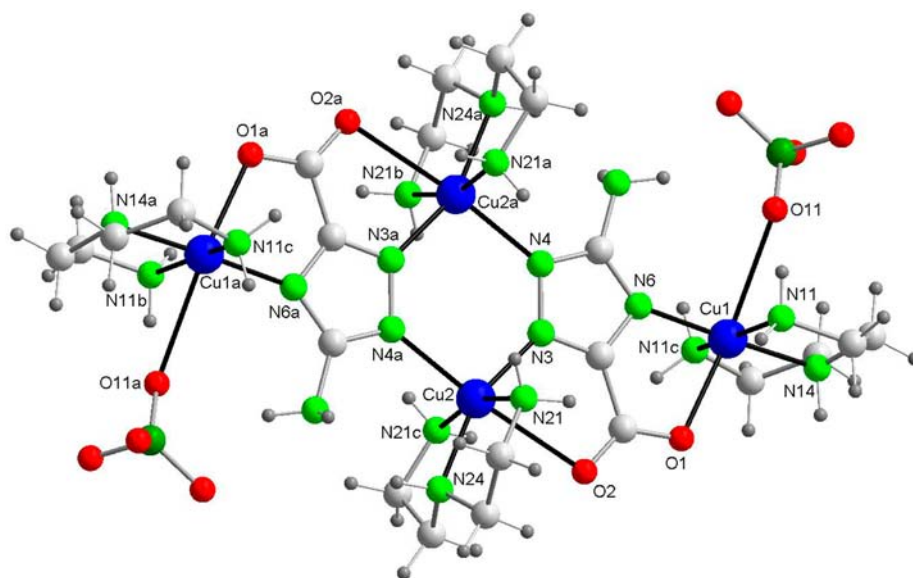


Figure 1. Plot of the tetranuclear cation of **1** showing the numbering scheme. Symmetry codes, a: $-x, y, -z$; b: $-x, -y, -z$; c: $x, -y, z$.

Table 1. Selected Bond Lengths and Angles for $[\text{Cu}_4(\text{atc})_2(\text{dien})_4(\text{ClO}_4)_2](\text{ClO}_4)_2 \cdot 2\text{H}_2\text{O}$ (**1**)^a

bond pair	bond distance (Å)	bond pair	bond distance (Å)
Cu(1)–N(14)	1.988(3)	Cu(2)–N(3)	1.996(4)
Cu(1)–N(11)	2.003(3)	Cu(2)–N(24)	2.025(4)
Cu(1)–N(11) ^c	2.003(3)	Cu(2)–N(21) ^c	2.034(3)
Cu(1)–N(6)	2.003(3)	Cu(2)–N(21)	2.034(3)
Cu(1)–O(1)	2.291(4)	Cu(2)–N(4) ^b	2.214(4)
Cu(1)–O(11)	2.704(5)	Cu(2)–O(2)	2.674(3)
Cu(1)–Cu(2)	5.6860(7)	Cu(2)–Cu(2) ^b	4.0588(10)
	bond angle (deg)		bond angle (deg)
N(14)–Cu(1)–N(11)	84.48(10)	N(3)–Cu(2)–N(24)	157.90(16)
N(14)–Cu(1)–N(11) ^c	84.48(10)	N(3)–Cu(2)–N(21) ^c	94.21(11)
N(11)–Cu(1)–N(11) ^c	165.9(2)	N(24)–Cu(2)–N(21) ^c	83.10(11)
N(14)–Cu(1)–N(6)	178.02(14)	N(3)–Cu(2)–N(21)	94.21(11)
N(11)–Cu(1)–N(6)	95.36(10)	N(24)–Cu(2)–N(21)	83.10(11)
N(11) ^c –Cu(1)–N(6)	95.36(10)	N(21) ^c –Cu(2)–N(21)	162.0(2)
N(14)–Cu(1)–O(1)	103.29(13)	N(3)–Cu(2)–N(4) ^b	100.76(14)
N(11)–Cu(1)–O(1)	95.55(14)	N(24)–Cu(2)–N(4) ^b	101.34(15)
N(11) ^c –Cu(1)–O(1)	95.55(14)	N(21) ^c –Cu(2)–N(4) ^b	97.03(9)
N(6)–Cu(1)–O(1)	78.69(13)	N(21)–Cu(2)–N(4) ^b	97.03(9)
N(14)–Cu(1)–O(11)	86.78(14)	N(3)–Cu(2)–O(2)	73.41(12)
N(11)–Cu(1)–O(11)	71.87(18)	N(24)–Cu(2)–O(2)	84.50(13)
N(11) ^c –Cu(1)–O(11)	98.73(18)	N(21) ^c –Cu(2)–O(2)	83.58(9)
N(6)–Cu(1)–O(11)	91.29(14)	N(21)–Cu(2)–O(2)	83.58(9)
O(1)–Cu(1)–O(11)	163.28(12)	N(4) ^b –Cu(2)–O(2)	174.16(12)

^aSymmetry codes: b, $-x, -y, -z$; c, $x, -y, z$.

The resulting solutions were incubated for 1 h at 37 °C; a quench buffer solution (4 μL) consisting of bromophenole blue (0.25%), xylenecyanole (0.25%), and glycerol (30%) was added. Next, the solution was subjected to electrophoresis on 0.8% agarose gel in 0.5 \times TBE buffer (0.045 M Tris, 0.045 M boric acid, and 1 mM EDTA) containing 2 $\mu\text{L}/100$ mL of a solution of EB (10 mg/mL) at 80 V for 2 h. The bands were photographed on a capturing system (Gelprinter Plus TDI). A correction factor of 1.31 was used for supercoiled DNA because the intercalation between EB and Form I DNA is relatively weak compared to that of nicked (Form II) and linear (Form III) DNA.^{27c} The fraction of each form of DNA was calculated by dividing the intensity of each band by the total intensities of all bands in the lane.

In order to investigate the contribution of electrostatic interactions in the plasmid DNA cleavage promoted by complex **1**, assays were conducted as described above but with an increase in the ionic strength of the reaction media by the addition of NaCl (from 0 to 300 mM).

To test for the presence of reactive oxygen species (ROS) generated during strand scission and for possible complex-DNA interaction sites, various reactive oxygen intermediate scavengers and groove binders were added to the reaction mixtures. The scavengers used were 2,2,6,6-tetramethyl-4-piperidone (0.4 M), Tiron (10 mM), and potassium iodide (0.4 M). In addition, a chelating agent of copper(I), neocuproine (175 μM), along with the groove binders Methyl Green (1.25 $\mu\text{g}/\text{L}$) and distamycin (12 μM) were also assayed. Samples were treated as described above.

Finally, the kinetic study of the cleavage was performed at different times with plasmid pUC18, which was incubated at 37 °C with 5 μM complex **1** (with 10-fold excess of ascorbate). Samples were treated as described above but quenched by placing on ice and adding loading dye. Time-dependent supercoiled and nicked DNA concentration data were fit to a first-order consecutive model defined by eq 1, where S corresponds to the concentrations of supercoiled plasmid, S_0 corresponds to the initial concentration, and k_{obs} corresponds to the observed first-order rate constants of DNA nicking.^{6a,b} Observed rate constant was expressed as min^{-1} .

$$S = S_0 \exp(-k_{\text{obs}}t) \quad (1)$$

All of the results are the average of experiments performed at least in triplicate.

RESULTS AND DISCUSSION

The ligand. The small H_2atc (5-amino-1,2,4-triazole-3-carboxylic acid) (Scheme 1a) ligand is hardly soluble in usual organic solvents and in water. To our knowledge, only a few coordination complexes of this ligand have been reported until now, the monomers of $\text{Cd} [\text{Cd}(\text{Hatc})_2(\text{H}_2\text{O})_2]^{28a}$ and $[\text{Cd}(\text{Hatc})_4][(\text{NH}_4)_2]^{28b}$ and some polymers of Dy, Ba, and Sr.²⁹

The 1,2,4-triazole derivatives are versatile ligands.¹² In complex **1**, the ligand is doubly deprotonated (atc^{2-}) by loss of the triazole H atom and the carboxylic H atom, thus offering six donor atoms for coordination and several bridges: $\mu\text{-N}1, \text{N}2$ -triazolato, $\mu\text{-N}2, \text{N}4$ -triazolato (or $\mu_3\text{-N}1, \text{N}2, \text{N}4$ -triazolato) and $\mu\text{-O}, \text{O}'$ -carboxylato (see in Scheme 1b usual bridging modes of 1,2,4-triazole ligands, taken from ref 12a). In the presence of the coligand dien (dien = diethylenetriamine = 1,4,7-triazahexane = 3-azapentane-1,5-diamine), the combination of those features has allowed us to isolate the simple “1 + 2 + 1” tetrameric Cu(II) compound which is described below.

Crystal Structure of $[\text{Cu}_4(\text{atc})_2(\text{dien})_4(\text{ClO}_4)_2] \cdot (\text{ClO}_4)_2 \cdot 2\text{H}_2\text{O}$ (1**).** The crystal structure of **1** is built up from $[\text{Cu}_4(\text{atc})_2(\text{dien})_4(\text{ClO}_4)_2]^{2+}$ cations, two noncoordinated perchlorate anions per cation and two lattice water molecules per cation. The cationic unit is depicted in Figure 1, together with the numbering scheme. Selected bond distances and angles are listed in Table 1.

The cationic complex can be described as a tetranuclear $\text{Cu}'\cdots\text{Cu}(\text{N}-\text{N})_2\text{Cu}\cdots\text{Cu}'$ copper(II) species with two types of metallic centers, Cu and Cu', doubly connected by $\mu\text{-N}2, \text{N}4$ -triazolato (in this structure: $\mu\text{-N}(3), \text{N}(6)$ -triazolato) and $\mu\text{-O}, \text{O}'$ -carboxylato bridges; the two equivalent Cu centers are linked by two $\mu\text{-N}1, \text{N}2$ -triazolato (here, $\mu\text{-N}(3), \text{N}(4)$ -triazolato) bridges. Following the CSD-CCDC database (release Feb12),²⁵ **1** represents the second case among the triazole or tetrazole complexes of a tetranuclear “1 + 2 + 1” copper(II) structure constructed by *discrete* units (i.e., nor catena neither 2D/3D polymer). Presumably, the dien coligand blocks the formation of an extended network, as is habitual for systems with tridentate $\text{N}1, \text{N}2, \text{N}4$ -triazolato ligands [related compounds, but made of *catena*, are described in refs 15a and 18].

Figure 1 and Figure S1 in the Supporting Information show how the two Cu(2) and Cu(2a) metal ions, related by an inversion center and doubly bridged by the triazolato N(3)–N(4) atoms of two atc^{2-} ligands, afford a central *dimeric* unit, common for 1,2,4-triazole ligands with chelating substituents.^{12a} Cu(2)/Cu(2a) are further connected to the *single* Cu(1)/Cu(1a) metal ions through the N(3)–C(2)–N(6)/N(3a)–C(2a)–N(6a) atoms of the μ_3 -triazolato ring and the O(1)–C(1)–O(2)/O(1a)–C(1a)–O(2a) atoms of the μ -carboxylate

substituent. In summary, atc^{2-} acts as a “ $\mu_3 + \mu_2$ ” pentadentate bis-chelating ligand.

The *central* Cu atoms exhibit a highly distorted octahedral environment constituted by two N atoms from two distinct triazolato rings, the three N atoms of a chelating dien ligand and one O carboxylate atom of an atc^{2-} ligand. Commonly, in the dinuclear structures of the bis-($\text{N}1, \text{N}2$ -triazole) systems the two Cu–N bond distances are similar, and range from 1.94 Å to 2.01 Å.^{30,31} In **1**, however, the double bridge is asymmetrical with one typical Cu(2)–N(3) [1.996(4) Å] and one long Cu(2)–N(4a) [2.214(4) Å] bond distances (see Figure S2). The asymmetry is also reflected in the Cu(2)–N(3)–N(4) and Cu(2)–N(4a)–N(3a) angles, with values of 134.42(19)° and 124.83(19)°, respectively. The Cu(2)–Cu(2a) bond distance, of 4.059(2) Å, does lie in the interval expected for symmetrical Cu–(N–N)₂–Cu systems. As for the Cu–N(dien) bond distances, the three of them are short and nearly equal [2.003–2.025–2.034(4) Å]. Finally, the long Cu–O(carboxylato) bond length [2.674(3) Å] is characteristic of a semicoordination. Thus, the octahedron bond distances taken into account, it could be considered that the Cu(2) equatorial plane is formed by the three N dien atoms and the N(3) triazolato atom; the apical positions are (*unusually*) occupied by the N(4) triazolato atom and the O(2) carboxylate one. The resulting chromophore is $\text{CuNN}'_3 + \text{N} + \text{O}$, with the Cu(2) atom shifted 0.316(3) Å out of the plane defined by the 4 basal donor atoms (Figure S2). The coordination angles are also far from the ideal 90° value, varying from 83.10(11)° to 97.03(9)° in the equatorial plane, and from 73.41(12)° to 101.34(15)° on apical positions. The distortion in angles is related with the formation of three chelating rings.

The coordination geometry around the *peripheral* Cu' center is also a distorted octahedron. In a way similar to Cu(2), the Cu(1) atom is equatorially bound by the three N atoms of the terminal dien ligand and by the single (not diazinic) N(6) atom of the triazolato ring with bond distances between 1.988(3) Å and 2.003(3) Å. The second O atom of the chelating carboxylato group is on apical position at 2.291(3) Å. The sixth site of the octahedron is occupied by the perchlorate O(11) atom which approaches Cu(1) at a semibonding distance of 2.704(5) Å. The chromophore of Cu(1) can be condensed as $\text{CuNN}'_3 + \text{O} + \text{O}'$, with the Cu(1) atom only deviated by 0.095(4) Å from its equatorial coordination plane (Figure S2). The bonding angles are in the range of 84.48(10)°–95.55(14)° in the basal plane, and 71.78(18)°–103.29(13)° on axial positions. The two bite angles of the carboxylato substituent are slightly different; that with Cu(2) (dimeric unit) is 73.41(12)°, and that with the external Cu(1) atom is 78.69(13)°.

The Cu(1)–Cu(2)/Cu(1)–Cu(2a) distances are 5.686 (1) and 6.370(1) Å, respectively. The entire cation is planar because of the symmetry of the structure, except for the N(11)–C(11)–C(12)/N(21)–C(22)–C(23) dien atoms and three out of four oxygen atoms of the perchlorate anions. The basal plane around the peripheral Cu(1) metallic center [defined by N(6), N(11), N(11c), and N(14)] and the plane defined by the bridging [Cu(2)(N–N)₂Cu(2a)] system are mutually perpendicular (Figure S1). Finally, the two external Cu(1) and Cu(1a) atoms are separated by 11.373(1) Å. In the compound described by Brooker et al., the 1,2,4-triazole ring is substituted on N4 and so the peripheral Cu' is not directly bound to the triazole ring but instead to the amino nitrogen atom of the N4-substituent; the resulting structure is not

planar, the Cu...Cu' distances are 6.300(1) and 7.355(1) Å, and the Cu'...Cu' separation is 13.026(2) Å.^{17a}

In the crystal structure, the tetranuclear building blocks self-assemble into a tridimensional hydrogen-bonded network. There are three main sets of H-bonds: (i) intramolecular, involving N(24)–N(7) and N(7)–O(13) atoms; (ii) intermolecular, through N(14)–O(1*) and O(1)–N(14*) atoms, which originate *chains of tetramers*, with Cu(1)...Cu(1*) distances of 5.420 Å (Figure S3a); and (iii) *interchain* intermolecular, through O(13)–N(11*) and N(11)–O(13*) atoms ("*" indicates that the atom belongs to a neighboring tetranuclear unit) (Figure S3a). The hydrogen bond parameters are compiled in Table S2. The result can be considered a metal–organic 3D framework which contains sheets parallel to the plane (–2 0 1) (Figure S3b). To be noticed, as mentioned earlier, that the presence of the coligand dien is crucial, since it presumably prevents the polymerization characteristic of the N1,N2,N4 bridging mode of the 1,2,4-triazole systems. A similar situation has been reported for the $\{[\text{Cu}_3(\text{tcz})_2(\text{dien})(\text{H}_2\text{O})_2] \cdot 3\text{H}_2\text{O}\}_n$ [tcz = 3,5-bis(carboxylato)-1,2,4-triazolato] compound.³²

Spectroscopic Characterization. Magnetic Properties of 1. The temperature dependence of the $\chi_M T$ product (χ_M being the magnetic susceptibility per tetranuclear unit) for complex **1** is shown in Figure 2. At room temperature, the $\chi_M T$ value is

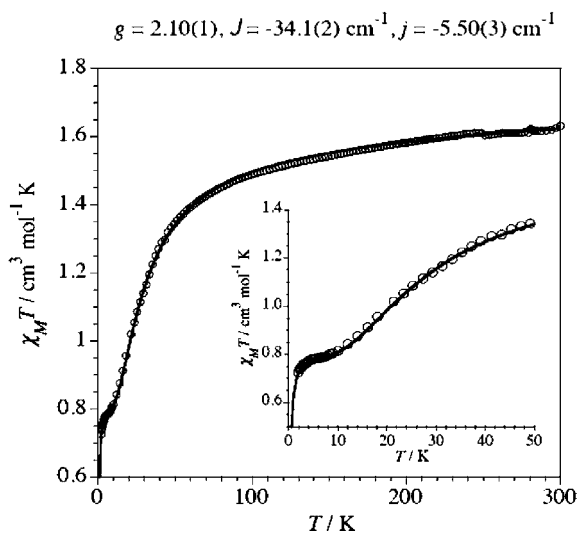
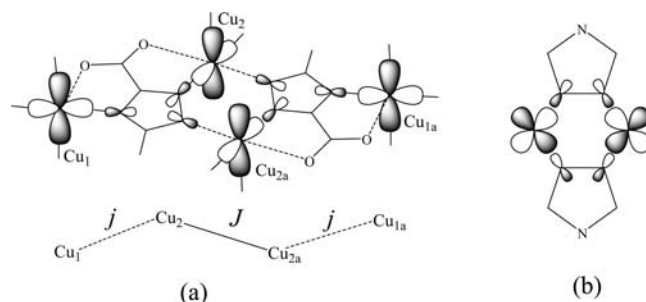


Figure 2. Experimental (○) and calculated (solid line) $\chi_M T$ vs T curve for **1** (χ_M being the magnetic susceptibility per tetranuclear unit).

close to $1.6 \text{ cm}^3 \text{ K mol}^{-1}$ (ca. $0.4 \text{ cm}^3 \text{ K mol}^{-1}$ per copper). No maximum is observed in the χ_M curve. The values of $\chi_M T$ decrease down to an incipient plateau of $\sim 0.8 \text{ cm}^3 \text{ mol}^{-1} \text{ K}$ in the 10–5 K temperature range. This value is close to that expected for two isolated $S = 1/2$ ground states with a reasonable g -value. Below this temperature $\chi_M T$ decreases continuously until $0.7 \text{ cm}^3 \text{ mol}^{-1} \text{ K}$. This behavior is in agreement with the presence of two *coupled* Cu(II) centers with a moderate-to-low antiferromagnetic interaction plus two *weakly coupled* Cu(II) centers with a very low antiferromagnetic interaction (so *almost isolated*).

The magnetic data have been interpreted by taking into account the structure of the tetranuclear complex. Scheme 2a shows the magnetic orbitals involved in the superexchange. The corresponding spin Hamiltonian is given in eq 2:

Scheme 2



$$\mathbf{H} = -J\mathbf{S}_2\mathbf{S}_{2a} - j(\mathbf{S}_1\mathbf{S}_2 + \mathbf{S}_{2a}\mathbf{S}_{1a}) \quad (2)$$

An exact matrix diagonalization by using MAGPAK³³ allowed us to calculate the J , j , and g magnetic parameters. In the fitting procedure, the g values were assumed to be the same for all Cu(II) ions. The best-fit parameters were $g = 2.10(1)$, $J = -34.1(2) \text{ cm}^{-1}$, and $j = -5.50(3) \text{ cm}^{-1}$. The solid line in Figure 2 corresponds to the theoretical curve obtained from these parameters.

In general, the magnetic coupling between two Cu(II) ions through double N1,N2-triazole bridges across the sigma in-plane exchange pathway (Scheme 2b) is large (J ca. -200 cm^{-1}).^{30,31} In the case of the reversal orbital situation shown in Scheme 2a, however, the overlap between the magnetic orbitals is much reduced due to their quasi-orthogonality and then, a very small magnetic coupling is expected. In addition, in **1**, the low symmetry of the involved bridging system favors the occurrence of the small net overlap. The result is a poor antiferromagnetic Cu(2)–Cu(2a) coupling ($J = -34 \text{ cm}^{-1}$). In the “1 + 2 + 1” Brooker’s compound a J value as low as $-6.8(8) \text{ cm}^{-1}$ [$g = 2.17(5)$] was obtained for the central coppers;^{17a} apparently, the two external coppers are so *isolated* that any j parameter was needed to reproduce the experimental magnetic data.

For N1,N2-triazole bridged copper(II) dimers, an empirical relation between the J value and the Cu–N–N^{30b}/N–Cu–N³¹ angles of the bridge has been reported. Following this correlation, the J value of **1** should be low, as found here experimentally. With respect to the magnitude of the j value (very low), the lack of comparable experimental (N–C–N_{triazole})-bridge values does not allow a proper discussion.^{34a} For the (N–C–N_{imidazole})-bridge, no simple magneto-structural correlation between geometric parameters and J could be found.^{34b} Further crystallographic and magnetic data are necessary to clarify the magnitude of the exchange in these triatomic bridges.

EPR of 1. Figure S4 displays the X-band EPR spectra on polycrystalline samples of **1** at different temperatures. In the entire range of temperatures (10–300 K), the spectra is quasi-isotropic ($g \approx 2.096$) or slightly axial. When cooling the sample, the signal becomes more intense in agreement with the experimental χ_M curve.

Solution Properties. Complex **1** exhibits a high solubility in water, which allows the investigation of **1** in aqueous solution. The UV–vis and EPR spectra (at 80 K) of **1** in solution (see Figures S9 and S4), as well as the conductivity measurements (with values close to the 1:2-electrolyte behavior), evidence that **1** is present as a whole tetranuclear entity in aqueous solution (ESI-MS analysis of **1**, both in low- and high-resolution modes were nonconclusive).

DNA Binding and DNA Cleavage Properties. DNA binding is the critical step for DNA cleavage in most cases. Therefore, interaction of complex **1** with CT-DNA was studied by fluorescence, thermal denaturation, and viscometric experiments. In general, DNA binding affinity is governed by one or more factors that include electrostatic interaction to the phosphate backbone, intercalation, and/or H-bonding.^{6a}

Fluorescence Spectral Studies—Competitive EB Displacement Assays. Fluorescence spectral technique is an effective method to study metal interaction with DNA. Ethidium bromide (EB) is one of the most sensitive fluorescence agents that can bind to DNA.^{10e,35} The fluorescence of EB increases after intercalating into DNA because of its burial in the hydrophobic region of DNA. The addition of a second DNA-binding molecule can quench the DNA-EB adduct emission by either replacing the EB and/or by accepting the excited-state electron of the EB.³⁶

Tetranuclear Cu(II) complex **1** (in different amounts) was added to DNA (fixed amount), pretreated with EB. Complex **1** causes an important reduction in fluorescence intensity, although without reaching the basal level (Figure 3). This

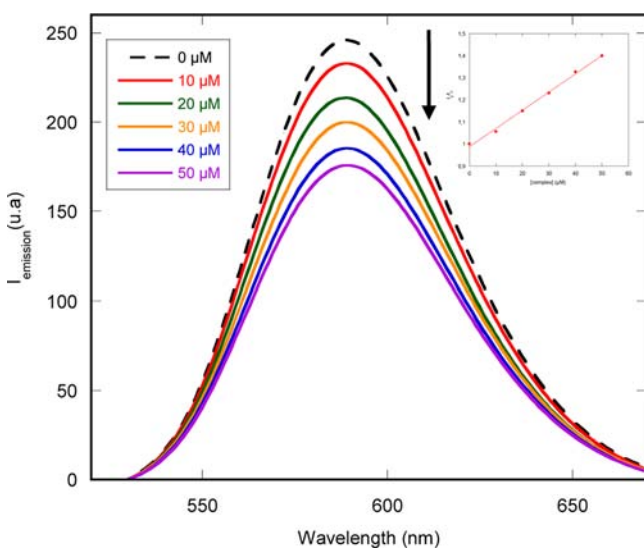


Figure 3. Emission spectra of EB bound to CT-DNA in the absence (dotted line) and presence (continuous lines) of **1**. The arrow shows the changes in intensity at increasing concentrations of the complex. Inset: Stern–Volmer graph. ([CT-DNA] = [EB] = 50 μM.)

indicates the partial removal of EB from DNA molecules due to the interaction of the complex with the DNA. The relative binding propensity was determined by the classical Stern–Volmer equation (eq 3):³⁷

$$\frac{I_0}{I} = 1 + K_{SV}[Q] \quad (3)$$

where I_0 and I are the fluorescence intensities of the CT-DNA in the absence and presence of complex **1**, respectively, K_{SV} is the Stern–Volmer dynamic quenching constant and $[Q]$ is the concentration of the quencher (in this case, complex **1**). In the linear fit plot of I_0/I versus $[Q]$ (or $[complex]$), K_{SV} is given by the ratio of the slope to intercept. The fluorescence quenching curve of DNA-bound EB by complex **1** is in good agreement with the linear Stern–Volmer equation ($R^2 = 0.996$). The K_{SV} value of complex **1** was calculated as $8.2 \times 10^3 \text{ M}^{-1}$.

An alternative way of expressing the degree of affinity toward DNA is the determination of the apparent binding constant, K_{app} , through a quantitative titration method that measures the concentration of an agent needed for 50% displacement of an initially bound EB (C_{50} value). This indirect fluorescent-based competition technique facilitates the determination of the “apparent” equilibrium constants for drug binding, since the C_{50} value is approximately inversely proportional to the binding constant.^{5c,38} The apparent binding constant K_{app} of **1** was calculated from eq 4:³⁷

$$K_{EB} \times [EB] = K_{app} \times [complex] \quad (4)$$

in which the complex concentration is the value at a 50% reduction of the fluorescence intensity of EB ($[EB] = 3.78 \mu\text{M}$) and $K_{EB} = 3.0 \times 10^7 \text{ M}^{-1}$ (calculated at pH 6.0 in this work). The K_{app} value obtained is $2.07 \times 10^6 \text{ M}^{-1}$.

In order to establish the relative magnitude of this K_{app} value, competitive EB displacement assays were simultaneously conducted with selected compounds: the intercalator acridine, the minor groove binder Hoechst 33258, the major groove binder Methyl Green, and CuSO_4 .

Figure 4 illustrates the different DNA-binding affinities. The C_{50} and K_{app} values are listed in Table 2. In the assay, the

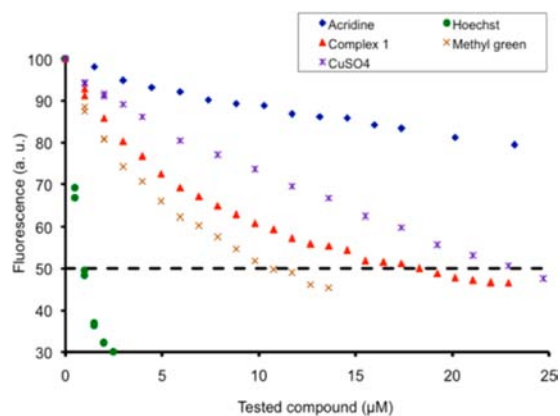


Figure 4. Competitive EB displacement assays with CT-DNA for acridine, Hoechst 33258, Methyl Green, CuSO_4 , and complex **1**. ([CT-DNA] = 3 μM; [EB] = 3.78 μM.)

Table 2. Apparent DNA Binding Constants (K_{app}) Evaluated for Complex **1** and Selected Compounds in This Work

compound	C_{50}^a (μM)	K_{app}^b [$\text{M}(\text{bp})^{-1}$]
Hoechst 33258	0.97	1.17×10^8
Methyl Green	10.93	1.04×10^7
complex 1	18.30	6.20×10^6
CuSO_4	23.15	4.90×10^6
acridine	75.85	1.50×10^6

^a C_{50} = concentration required to reduce fluorescence by 50%. ^b $K_{app} = K_{EB} \times 3.78 / C_{50}$, where $K_{EB} = 3 \times 10^7 \text{ M}(\text{bp})^{-1}$ (pH 6.0).

acridine shows a modest K_{app} value, as reported for other intercalating agents,^{5c,38} Hoechst 33258 is the most efficient in the displacement of DNA-bound EB and, comparably, complex **1**, Methyl Green, and CuSO_4 have lower, but still important, K_{app} values.

Thermal Denaturation Assays. The interaction of complex **1** with CT-DNA has also been characterized by measuring its

effect on the *melting temperature* (thermal denaturation experiment) of DNA. The stabilizing effect of complex **1** was investigated until complete saturation conditions (i.e., at $[DNA]/[complex]$ ratios from 2 to 8) and at low ionic strength (1 mM phosphate buffer 2 mM NaCl), in order that the melting transitions could be observed at moderate temperatures. The T_m curve is displayed in Figure 5. An

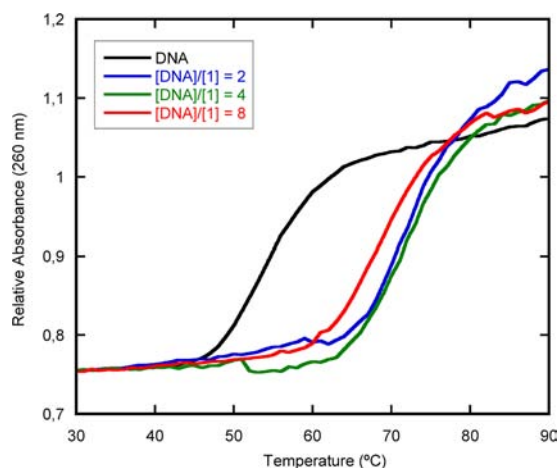


Figure 5. DNA melting temperature dependence on complex concentration: (black line) CT–DNA 100 μ M in the absence of complex; (colored lines) CT–DNA 100 μ M in the presence of 12.5–25–50 μ M of complex **1** [1 mM phosphate buffer, pH 7.2, $I = 2$ mM NaCl]. Legend: ratio $[DNA]/[complex \mathbf{1}]$.

important increase in the melting temperature is observed ($\Delta T_m = 18.3$ °C at $r = 4$), indicative of stabilization of the double-stranded nucleic acids by the metal complex. Mao et al. for copper complexes of a 2,2-dipyridyl ligand with guanidinium/ammonium pendants (therefore, cationic) have reported ΔT_m values ranging from 9.4 °C to 3.3 °C (pH 8.0, $I = 0.1$ M, $r = 0.2$).³⁹ Thus, the findings of this work show that complex **1** binds tightly to DNA.

Viscosity Measurements. In order to clarify the binding mode of complex **1** with DNA, the viscosity of DNA solutions containing varying amounts of added complex was measured. The experiment involves the measurement of the flow rate of DNA solution through a capillary viscometer. A classical intercalation model demands that the DNA helix lengthens as base pairs are separated to accommodate the binding ligand, leading to the increase of DNA viscosity. Well-known DNA intercalators, such as EB, give rise to a significant change in DNA viscosity upon complexation.³⁷ By contrast, $Cu^{2+}(aq)$ or drug molecules that bind either in the sugar–phosphate backbone or in the DNA grooves (e.g., netropsin, distamycin), under the same conditions essentially exert no such effect or cause only small (positive or negative) changes in DNA solution viscosity.⁴⁰ The effects of complex **1** on the viscosity of CT-DNA are shown in Figure S5. The results indicate that the presence of complex **1** does not modify the relative viscosity of CT-DNA and then, that the binding does not involve a classic intercalation, probably because of the lack of fused aromatic rings. Compound **1** rather binds either in DNA grooves or in the sugar–phosphate backbone.

DNA Cleavage Activity. (i). *Cleavage of Supercoiled pUC18 DNA (37.5 μ M bp) by the Complex 1.* **1** was examined following the conversion of pUC18 supercoiled DNA (Form I) to the open circular (Form II) and linear (Form III) DNA,

using agarose gel electrophoresis to separate the cleavage products (see Figure 6).

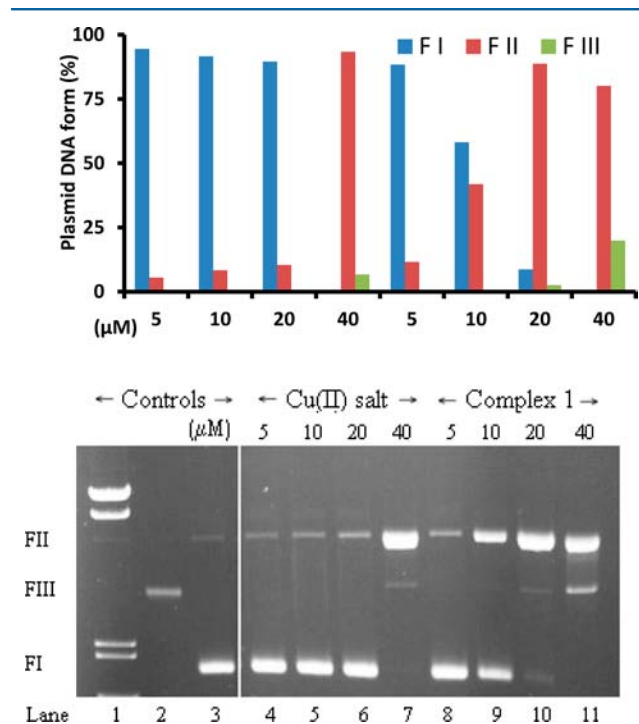


Figure 6. Cleavage of supercoiled DNA by complex **1**, where $[pUC18 \text{ DNA}] = 37.5$ μ M (bp), $[complex \mathbf{1}] = 5\text{--}40$ μ M, $[ascorbate] = 2.5$ -fold (0.625-fold per copper), cacodylate buffer (pH 6.0), for 60 min at 37 °C. Lane 1, marker; lane 2, linear DNA control; lane 3, DNA control; lane 4, 5 μ M $CuSO_4$ (12.5/4 μ M ascorbate); lane 5, 10 μ M $CuSO_4$ (25/4 μ M ascorbate); lane 6, 20 μ M $CuSO_4$ (50/4 μ M ascorbate); lane 7, 40 μ M $CuSO_4$ (100/4 μ M ascorbate); lane 8, 5 μ M complex **1** (12.5 μ M ascorbate); lane 9, 10 μ M complex **1** (25 μ M ascorbate); lane 10, 20 μ M complex **1** (50 μ M ascorbate); lane 11, 40 μ M complex **1** (100 μ M ascorbate). The bottom panel shows the gel image; the top panel shows the relative concentrations of supercoiled, nicked, and linear form for Cu(II) salt 5–40 μ M (left) (see ascorbate-only control in Figure S8) and complex **1** 5–40 μ M (right).

The complex was found to exhibit concentration-dependent cleavage of SC DNA, with almost complete degradation of the supercoiled form (8%) to produce the open circular (89%) and linear (3%) forms at concentrations as low as 20 μ M in the presence of a mild reducing agent (ascorbate, 2.5 \times) and dioxygen (lane 10) but not under hydrolytic conditions (lacking activating agent, data not shown). At 40 μ M, the compound induced complete degradation of the supercoiled form to produce the open circular (80%) and linear (20%) forms (lane 11), indicating that the complex is indeed an efficient chemical nuclease. Control experiments, in equal reaction conditions but replacing the complex by $CuSO_4$ (plus the same fold of ascorbate *per copper*), were carried out in parallel. The comparison of reactivity revealed that complex **1** (10 μ M, lane 9) is more active than $CuSO_4$ (10 μ M, lane 5) but less active than equimolar Cu(II) in copper salt (40 μ M, lane 7). This finding, which could be related to the lack of labile coordination positions on the central coppers, rules out a possible synergistic effect between the different copper centers in complex **1**.

(ii). *Ionic Strength Dependence of DNA Cleavage Promoted by 1.* The influence of electrostatic properties of

complex **1** on the plasmid DNA cleavage was analyzed by the addition of increasing amounts of NaCl in a range 0–300 μM to the reaction medium (Figure S6). When NaCl is added, a proportional decrease of the plasmid DNA cleavage promoted by **1** is observed. This effect was somehow expected. Since **1** behaves as cation in solution, the increase in salt concentration must neutralize negative charges in DNA, which decreases the electrostatic attraction between the complex and DNA. This result is evidence for the contribution of electrostatic interactions to the DNA binding event.^{5a}

(iii). **DNA Cleavage Mechanism.** In order to identify the mechanistic aspects of the complex activity, control experiments were carried out in the presence of ROS scavengers (Figure 7). In the presence of potassium iodide (lane 6),

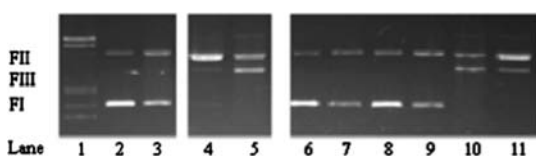


Figure 7. Effect of ROS scavengers and groove binders on the cleavage of supercoiled DNA by complex **1**, where [pUC18 DNA] = 37.5 μM (bp), cacodylate buffer (pH 6.0), for 60 min at 37 °C. Lane 1, marker; lane 2, DNA control; lane 3, DNA + 360 μM ascorbate; lanes 4 and 5, 18–20 μM complex **1** (+ 360–400 μM ascorbate); lanes 6–11 contain complex **1** 20 μM (+ 400 μM ascorbate) plus added agent: lane 6, KI, lane 7, 2,2,6,6-tetramethyl-4-piperidone; lane 8, Tiron; lane 9, neocuproine; lane 10, distamycin; and lane 11, Methyl Green.

2,2,6,6-tetramethylpyridone (lane 7) and Tiron (lane 8), the plasmid DNA cleavage was fully inhibited (compare with lanes 4 and 5). This suggests the participation of hydroxyl ($\cdot\text{OH}$), singlet-oxygen ($^1\text{O}_2$), and superoxide (O_2^-) radicals on the DNA breakage, thus confirming the oxidative nature of **1** as nuclease.

Since the oxidative mechanism of plasmid DNA cleavage by many metal complexes involves a metal center reduction, assays in the presence of neocuproine, a copper(I) chelator, were also performed. Upon addition of neocuproine, the plasmid DNA cleavage was inhibited (lane 9), which suggests the participation of copper(I) on the cleavage process.

Finally, no apparent inhibition of plasmid DNA cleavage was observed pretreating the plasmid neither with distamycin (minor groove binding agent), nor with Methyl Green (major groove binding agent) (lanes 10 and 11). These results match with the previously suggested electrostatic DNA interacting behavior through the phosphato groups and point to the nonspecificity in the DNA binding by **1**.

(iv). **Kinetic Assays.** The kinetics of pUC18 DNA degradation has been studied. Conditions of experiment have been purposely selected in order to observe gradual appearance/disappearance of each DNA form and to avoid smearing (fully DNA degradation) (Figure 8 (top)). The loss of supercoiled DNA and increased levels of open circular and linear DNA forms were quantified after gel electrophoresis, as described in the Experimental Section, and then fitted with the aid of the kinetic model proposed by Cowan.^{6b} The results are shown in Figure 8 (bottom). The extent of supercoiled DNA cleavage into nicked form promoted by **1** varies exponentially with the reaction time, giving pseudo-first-order kinetics with an apparent initial first-order rate constant (k_{obs}) of $\sim 0.126 \text{ min}^{-1}$ ($R^2 = 0.996$), which corresponds to a short half-life of 5.5 min for supercoiled DNA. These kinetic parameters (with a low

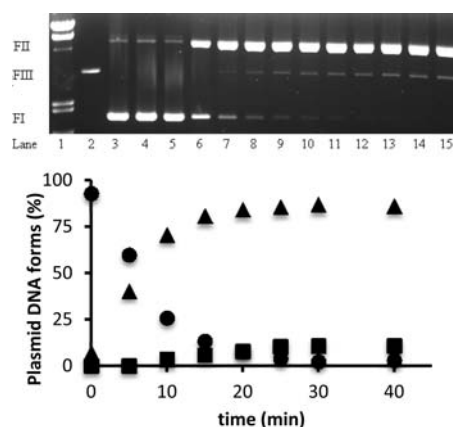


Figure 8. Kinetics of supercoiled DNA cleavage by complex **1**, where [pUC18 DNA] = 37.5 μM (bp), [complex **1**] = 5 μM , [ascorbate] = 50 μM , Tris buffer (pH 7.2), at 37 °C. Lanes: at (5) 0 min, (6) 5 min, (7) 10 min, (8) 15 min, (9) 20 min, (10) 25 min, (11) 30 min, (12) 40 min, (13) 50 min, (14) 60 min, and (15) 75 min; controls at 75 min: (1) marker, (2) linear DNA control, (3) DNA control, (4) DNA with 50 μM ascorbate. Top panel shows the gel image. Bottom panel shows the variation of the relative concentrations of (●) supercoiled, (▲) nicked, and (■) linear form.

concentration, 5 μM , of **1**) confirm the very high competence of this easy copper complex toward DNA damage.¹ Cowan already reported on the importance of binding affinity for efficient catalytic cleavage.^{6a} Mention should be done that, under the same experimental conditions (identical amount of ascorbate *per copper*), $\text{Cu}^{2+}(\text{aq})$ did not show DNA cleavage (see Figure S8).

CONCLUSION

This paper reports on the synthesis and characterization of a discrete “1 + 2 + 1” tetranuclear copper(II) compound, from the atc^{2-} ligand, which acts as $N1,N2$ bridge and $N2,O$ and $N4,O'$ double chelate. It represents a simple example of a new class of tetrameric coordination compounds. The magnetic study indicates that **1** exhibits an unusually (although predictable) weak antiferromagnetic coupling between the two central bis($N1,N2$)-bridged coppers centers, and a very weak antiferromagnetic coupling, through the $N2,C,N4$ -bridge, between each peripheral copper and one of the two central copper centers.

Its good solubility makes it suitable for the biological study. The complex binds to DNA with a high K_{app} , preferentially through electrostatic interactions, and then cleaves DNA strands by an oxidative mechanism involving generation of ROS in the presence of a mild reductant. Although no cooperative effect between copper centers has been appreciated, **1** shows a good reactivity toward DNA, most likely initiated by the attraction toward the phosphate backbone and followed by a nonspecific attack of DNA in multiple positions. The use of multinuclear Cu(II) complexes appears to be an alternative strategy for introducing several positively charged sites in the nuclease with the objective of improving its DNA binding. We are currently developing new related systems.

ASSOCIATED CONTENT

Supporting Information

Additional tables (S1,S2) and figures (S1–S9). This material is available free of charge via the Internet at <http://pubs.acs.org>.

AUTHOR INFORMATION

Corresponding Author

*E-mail: Sacramento.Ferrer@uv.es (S. F.).

Notes

The authors declare no competing financial interest.

ACKNOWLEDGMENTS

This work was supported by the Ministerio de Educación y Ciencia (MEC, Spain) (Project No. CTQ2007-6369/BQU). J.H.G. acknowledges for a Ph.D. grantship (Project No. CTQ2007-6369/BQU, MEC, Spain).

REFERENCES

- (1) Jiang, Q.; Xiao, N.; Shi, P.; Zhua, Y.; Guo, Z. *Coord. Chem. Rev.* **2007**, *251*, 1951–1972.
- (2) (a) Steinreiber, J.; Ward, T. *Coord. Chem. Rev.* **2008**, *252*, 751–766. (b) Mancin, F.; Scrimin, P.; Tecilla, P.; Tonellato, U. *Chem. Commun.* **2005**, 2540–2548.
- (3) (a) Desbouis, D.; Troitsky, I.; Belousoff, M.; Graham, B.; Spiccia, L. *Coord. Chem. Rev.* **2012**, *256*, 897–937 and references therein. (b) Liu, C.; Wang, M.; Zhang, T.; Sun, H. *Coord. Chem. Rev.* **2004**, *248*, 147–168. (c) Maheswari, P.; Roy, S.; den Dulk, H.; Barends, S.; van Wezel, G.; Kozlevcár, B.; Gámez, P.; Reedijk, J. *J. Am. Chem. Soc.* **2006**, *128*, 710–711.
- (4) (a) Pogozelski, W.; McNeese, T.; Tullius, T. *J. Am. Chem. Soc.* **1995**, *117*, 6428–6433. (b) Sigman, D. *Acc. Chem. Res.* **1986**, *19*, 180–186. (c) Claussen, C.; Long, E. *Chem. Rev.* **1999**, *99*, 2797–2816. (d) Fang, Y.; Claussen, C.; Lipkowitz, K.; Long, E. *J. Am. Chem. Soc.* **2006**, *128*, 3198–3207. (e) Czlapinski, J.; Sheppard, T. *Chem. Commun.* **2004**, 2468–2469.
- (5) (a) Silva, P.; Guerra, W.; Silveira, J.; Ferreira, A.; Bortolotto, T.; Fischer, F.; Terenzi, H.; Neves, A.; Pereira-Maia, E. *Inorg. Chem.* **2011**, *50*, 6414–6424. (b) Bortolotto, T.; Silva, P. P.; Neves, A.; Pereira-Maia, E.; Terenzi, H. *Inorg. Chem.* **2011**, *50*, 10519–10521. (c) Kellet, A.; O'Connor, M.; McCann, M.; McNamara, M.; Lynch, P.; Rosair, G.; McKee, V.; Creaven, B.; Walsh, M.; McClean, S.; Foltyn, A.; O'Shea, D.; Howe, O.; Devereux, M. *Dalton Trans.* **2011**, 1024–1027.
- (6) (a) Jin, Y.; Cowan, J. A. *J. Am. Chem. Soc.* **2005**, *127*, 8408–8415. (b) Joyner, J.; Reichfield, J.; Cowan, J. *J. Am. Chem. Soc.* **2011**, *133*, 15613–15626. (c) Sreedhara, A.; Cowan, J. *J. Biol. Inorg. Chem.* **2001**, *6*, 337–347. (d) Cowan, J. *Curr. Opin. Chem. Biol.* **2001**, *5*, 634–642.
- (7) Ferrer, S.; Ballesteros, R.; Sambartolomé, A.; González, M.; Alzuet, G.; Borrás, J.; Liu, M. *J. Inorg. Biochem.* **2004**, *98*, 1436–1446.
- (8) Dallavalle, F.; Gaccioli, F.; Franchi-Gazzola, R.; Lanfranchi, M.; Marchio, L.; Pellinghelli, M.; Tegoni, M. *J. Inorg. Biochem.* **2002**, *92*, 95–104.
- (9) (a) Humphreys, K.; Karlin, K.; Rokita, S. *J. Am. Chem. Soc.* **2002**, *124*, 8055–8066. (b) Li, L.; Karlin, K.; Rokita, S. *J. Am. Chem. Soc.* **2005**, *127*, 520–521.
- (10) (a) Bales, B.; Pitié, M.; Meuneir, B.; Greenberg, M. *J. Am. Chem. Soc.* **2002**, *124*, 9062–9063. (b) Tu, C.; Shao, Y.; Gan, N.; Xu, Q.; Guo, Z. *Inorg. Chem.* **2004**, *43*, 4761–4766. (c) Zhao, Y.; Zhu, J.; He, W.; Yang, Z.; Zhu, Y.; Li, Y.; Zhang, J.; Guo, Z. *Chem.—Eur. J.* **2006**, *12*, 6621–6629. (d) García-Giménez, J.; Alzuet, G.; González-Álvarez, M.; Castineiras, A.; Liu-González, M.; Borrás, J. *Inorg. Chem.* **2007**, *46*, 7178–7188. (e) Anbu, S.; Kandaswamy, M.; Kamalraj, S.; Muthumary, J.; Varghese, B. *J. Chem. Soc., Dalton Trans.* **2011**, 7310–7318.
- (11) Li, D.; Tian, J.; Gu, W.; Liu, X.; Yan, S. *J. Inorg. Biochem.* **2010**, *104*, 171–179.
- (12) (a) Haasnoot, J. *Coord. Chem. Rev.* **2000**, *200*, 131–185. (b) Klingele, M.; Brooker, S. *Coord. Chem. Rev.* **2003**, *241*, 119–132. (c) Aromí, G.; Barrios, L.; Roubeau, O.; Gámez, P. *Coord. Chem. Rev.* **2011**, *255*, 485–546.
- (13) Prins, R.; de Graaff, R.; Haasnoot, J.; Vader, C.; Reedijk, J. *J. Chem. Soc., Chem. Commun.* **1986**, 1430–1431.
- (14) (a) ten Hoedt, R.; Hulsbergen, F.; Verschoor, G.; Reedijk, J. *Inorg. Chem.* **1982**, *21*, 2369–2373. (b) Abarca, B.; Ballesteros, R.; Chadlaoui, M.; Ramirez de Arellano, C.; Real, J. *Eur. J. Inorg. Chem.* **2007**, 4574–4578. (c) Isele, K.; Franz, P.; Ambrus, C.; Bernardini, G.; Decurtins, S.; Williams, A. *Inorg. Chem.* **2005**, *44*, 3896–3906. (d) Mukherjee, A.; Raghunathan, R.; Saha, M.; Nethaji, M.; Ramasesha, S.; Chakravarty, A. *Chem.—Eur. J.* **2005**, *11*, 3087–3096. (e) Tercero, J.; Ruiz, E.; Álvarez, S.; Rodríguez-Forte, A.; Alemany, P. *J. Mater. Chem.* **2006**, *16*, 2729–2735. (f) Banerjee, A.; Singh, R.; Mondal, P.; Colacio, E.; Rajak, K. *Eur. J. Inorg. Chem.* **2010**, 790–798. (g) van Albada, G.; Ghazzali, M.; Al-Farhan, K.; Reedijk, J. *Inorg. Chem. Commun.* **2011**, *14*, 1149–1152.
- (15) (a) Zhang, J.; Lin, Y.; Huang, X.; Chen, X. *J. Am. Chem. Soc.* **2005**, *127*, 5495–5506. (b) Zhang, J.; Lin, Y.; Huang, X.; Chen, X. *Chem. Commun.* **2005**, 1258–1260. (c) Ray, A.; Mitra, S.; Rosair, G. *Inorg. Chem. Commun.* **2008**, *11*, 1256–1259.
- (16) Zhou, J.; Cheng, R.; Song, Y.; Li, Y.; Yu, Z.; Chen, X.; Xue, Z.; You, X. *Inorg. Chem.* **2005**, *44*, 8011–8022.
- (17) (a) Olgún, J.; Kalisz, M.; Clérac, R.; Brooker, S. *Inorg. Chem.* **2012**, *51*, 5058–5069. (b) We do not include here the compound [Cu(maamt)(CuCl₃)]₂ (maamt = 4-amino-3,5-bis(aminomethyl)-1,2,4-triazole), which contain mixed valence “1(I) + 2(II,II) + 1(I)” tetracopper units but constructed with two (Cu^ICl₃) groups: see van Koningsbruggen, P.; Haasnoot, J.; Kooijman, H.; Reedijk, J.; Spek, A. *Inorg. Chem.* **1997**, *36*, 2487–2489.
- (18) (a) Chen, D.; Liu, Y.; Lin, Y.; Zhang, J.; Chen, X. *Cryst. Eng. Commun.* **2011**, *13*, 3827–3831. (b) Zhu, A.; Xu, Q.; Liu, F.; Qi, X. *Z. Anorg. Allg. Chem.* **2011**, *637*, 502–505. (c) Zhong, D.; Lu, W.; Jiang, L.; Feng, X.; Lu, T. *Cryst. Growth Des.* **2010**, *10*, 739–746.
- (19) Bruker. APEX2 Software, V2.0-1; Bruker AXS, Inc.: Madison, WI, 2005.
- (20) Sheldrick, G. M. SADABS. *Program for Empirical Absorption Correction of Area Detector Data*; University of Goettingen, Germany, 1997.
- (21) Sheldrick, G. M. *Acta Crystallogr., Sect. A: Found. Crystallogr.* **1990**, *A46*, 467–473.
- (22) Sheldrick, G. M. SHELXL-97. *Program for the Refinement of Crystal Structures*; University of Goettingen, Goettingen, Germany, 1997.
- (23) Wilson, A. J. C. *International Tables for Crystallography, Vol. C*; Kluwer Academic Publishers: Dordrecht, The Netherlands, 1995.
- (24) Brandenburg, K.; Putz, H. DIAMOND 3.x; Crystal Impact GbR, Bonn, Germany, 2004.
- (25) Interface. *The Cambridge Structural Database, Release 5.33* (updates Feb 2012), Cambridge, UK, Cambridge, U.K.
- (26) Strothkamp, K. *J. Chem. Educ.* **1994**, *71*, 77–79.
- (27) (a) Wilson, W.; Tanious, F.; Fernandez-Saiz, M.; Rigl, C. In *Drug–DNA Interaction Protocols*; Fox, K. R., Ed.; Methods in Molecular Biology, Vol. 90; Humana Press: Totowa, NJ, 1997; Chapter 15, pp 219–240. (b) Wilson, W.; Ratmeyer, L.; Zhao, M.; Strekowski, L.; Boykin, D. *Biochemistry* **1993**, *32*, 4098–4104. (c) Van den Berg, T.; Feringa, B.; Roelfes, G. *Chem Commun.* **2007**, 180–182.
- (28) (a) Wang, J.; Li, W.; Wang, J.; Xiao, H. *Z. Kristallogr. NCS* **2011**, *226*, 163–164, DOI: 10.1524/ncrs.2011.007. (b) Siddiqui, K.; Mehrotra, G.; Narvi, S.; Butcher, R. *Inorg. Chem. Commun.* **2011**, *14*, 814–817.
- (29) (a) Sun, Y.; Xiong, G.; Guo, M.; Ding, F.; Wang, L.; Gao, E.; Zhu, M.; Verpoort, F. *Z. Anorg. Allg. Chem.* **2011**, *637*, 293–300. (b) Chen, Y.; Xu, J.; Wang, K.; Wang, Y. *Jiegou Huaxue (Chin. J. Struct. Chem.)* **2011**, *30*, 799.
- (30) (a) Slangen, P.; Van Koningsbruggen, P.; Goubitz, K.; Haasnoot, J.; Reedijk, J. *Inorg. Chem.* **1994**, *33*, 1121–1126. (b) Van Oudenniel, W.; de Graaff, R.; Haasnoot, J.; Prins, R.; Reedijk, J. *Inorg. Chem.* **1989**, *28*, 1128–1133.
- (31) Ferrer, S.; van Koningsbruggen, P.; Haasnoot, J.; Reedijk, J.; Kooijman, H.; Spek, A.; Lezama, L.; Arif, A.; Miller, J. *J. Chem. Soc.—Dalton Trans.* **1999**, 4269–4276.
- (32) Van Koningsbruggen, P.; Van Hal, J.; de Graaff, R.; Haasnoot, J.; Reedijk, J. *J. Chem. Soc.—Dalton Trans.* **1993**, 1371–1375.

- (33) Borrás-Almenar, J. J.; Clemente-Juan, J. M.; Coronado, E.; Tsukerblat, B. *J. Comput. Chem.* **2001**, *22*, 985–991.
- (34) (a) Engelfriet, D.; den Brinker, W.; Verschoor, G.; Gorter, S. *Acta Crystallogr., Sect. B: Struct. Crystallogr. Cryst. Chem.* **1979**, *35*, 2922–2927. (b) Pals, W.; Pohlmann, A.; Subramanian, P.; Srinivas, D. *Z. Anorg. Allg. Chem.* **2002**, *628*, 1377–1384.
- (35) Baguley, B.; Le Bret, M. *Biochemistry* **1984**, *23*, 937–943.
- (36) Selvakumar, B.; Rajendiran, V.; Uma Maheswari, P.; Stoeckli-Evans, H.; Palaniandavar, M. *J. Inorg. Biochem.* **2006**, *100*, 316–330.
- (37) Carter, M.; Rodriguez, M.; Bard, A. *J. Am. Chem. Soc.* **1989**, *111*, 8901–8911.
- (38) Jenkins, T. In *Drug–DNA Interaction Protocols*; Fox, K. R., Ed.; Methods in Molecular Biology, Vol. 90; Humana Press: Totowa, NJ, 1997; Chapter 14, pp 195–218.
- (39) He, J.; Hu, P.; Wang, Y.; Tong, M.; Sun, H.; Mao, Z.; Ji, L. *Dalton Trans.* **2008**, 3207–3214.
- (40) (a) Wu, J.; Yuan, L.; Wu, J. *J. Inorg. Biochem.* **2005**, *99*, 2211–2216. (b) Talib, J.; Harman, D.; Dillon, C.; Wright, J.; Becka, J.; Ralph, S. *Dalton Trans.* **2009**, 504–513.